PREDICTING THE COOLANT FLOW AND HEAT TRANSFER IN RADIAL TURBINE BLADES

Aidin Panahi[1,*] and Mozzafar Ali Mehrabian[2]
[1, 2] Mechanical Engineering Department
University of Kerman, Kerman, Iran
([*] Corresponding author: aidin.panahi@gmail.com)

ABSTRACT. In this investigation, a computer code for predicting the coolant flow behavior and determining the critical points in radial turbine blades was developed, which can be applied for analysis of heat conduction in those turbomachines their geometry only consists of an inlet and an exit. This code is capable of simulating stationary and rotating passages with rib turbulators, impingement in tip-cap and finned passages with different geometries when the mass flow rate is not constant and the control volume is non-adiabatic. If the entrance pressure, entrance temperature and exit pressure; or the inlet flow rate, entrance pressure and entrance temperature are selected as entry data, then, the pressure distribution, temperature distribution, velocity distribution, local heat transfer coefficient, friction factor and local mass flow rate are calculated by the code and would be available to the designer. The obtained results of the computer code for stationary and rotating passages are in good agreement with experimental results. Two-dimensional numeral analysis is carried out to simulate the stationary passage of turbine blade. The results are compared with the developed program in this research as well as with the experimental data. The results are within acceptable engineering error margin.

NOMENCLATURE

C_1, C_2, C_T	----	Constants
D	m	Diameter
$D_h = \frac{4A}{P}$	m	Hydraulic Diameter
$D_{h,v} = \frac{4v_{pin}}{S}$	m	Hydraulic Diameter based on open volume
e_1	m	Surface Roughness
e_2	m	Rib Height
$e^+ = \mathrm{Re}(e_2/D)\sqrt{f/2}$	----	Dimensionless Parameter
f	----	Friction Factor
H	m	Channel Height
h	J/kg	Enthalpy
h_c	$W/m^2.K$	Heat Transfer Coefficient
$j = h_c(\mathrm{Pr})^{2/3}/\rho v C_p$	----	Colburn J-factor
l	m	Interval Length
L_{imp}	m	Impingement Distance

L_f	m	Half Height of fin
m	kg	Mass
$\dot{m}$	kg/s	Mass Flow Rate
M	----	Mach Number
N	rpm	Rotational Speed
P	m	Perimeter
$Rs = N.D_h/V$	----	Rossby Number
r	m	Radius
SP	m	Inlet Hole Spacing
V	m/s	Velocity
v	m^3	Volume
W	m	Fin Spacing
w	m	Channel width
$X = (A_1/A_2)^{0.5}$	----	Dimensionless Parameter
x	m	Distance along Flow Path
y	m	Distance in plane perpendicular to others
z	m	Distance along axis of rotation
ρ^+	m	Rib Spacing
τ_f	m	Fin Thickness
$\varphi_f = (2h_{c,pp}/K\tau_f)^{0.5}$	----	Dimensionless Parameter

Subscripts

a	Adiabatic wall
imp	Impingement
inj	Injection
n	Node
ref	Reference
v	Open Volume
w	Wall
2	Station at tip-cap inlet
3	Station in tip-cap chamber
4	Station at tip-cap chamber

INTRODUCTION

There are great economical benefits due to operation of steam and gas turbines in high temperatures, but considering the mechanical properties of materials used in turbine structure, thermal limitations are applied, especially in turbine blades [1]. Blades must be cooled if significantly higher turbine inlet temperatures are desired. Optimum design of turbine blade requires an accurate analysis of critical points. Such analysis, can only be performed if pressure distribution and heat transfer coefficients within the blade are known. A computer program is developed to calculate the flow and heat transfer characteristics inside the coolant passage. A schematic diagram of the coolant passage inside the turbine blade is shown in figure 1.

It should be noted that to obtain a two-dimensional distribution of heat transfer coefficient in the plane of the blade surface will really require a three-dimensional analysis. Because of the complex nature of the flow field in cooling passages, it is extremely difficult to develop a generalized three-

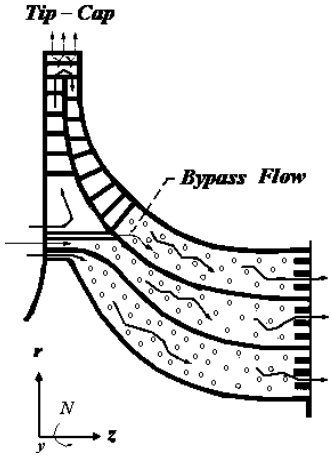

Figure 1. Sketch of cooled radial turbine configuration

dimensional code capable of modeling different cooling passage configurations and to calculate the flow and heat transfer characteristics. A need exists for a simple, one-dimensional screening code that can be used to narrow down the number of possible configurations in a timely manner.

The computer program integrates the one dimensional momentum and energy equations along a curvilinear path and calculates the coolant flow rate, temperature, pressure, velocity and heat transfer coefficient along the passage. No simplification was done to obtain the governing equations. The equations account for area change, mass addition or subtraction, pumping, friction and heat transfer. Flow can be bled off for tip cap impingement cooling and a flow bypass can be specified in which the coolant flow is taken off at one point in the flow channel and reintroduced at a point further downstream in the same channel. In order to increase the heat transfer coefficients in coolant passage, finned passages as shown in figure 1, were utilized.

El-Wakill [1] described calculations of a power plant technology. Steinthorsen *et al*. [2] were developed an explicit multiblock / multigrid flow solver for viscous flows in complex geometries. Also, Steinthorsen *et al*. [3] simulated a turbine cooling flows using a multiblock / multigrid flow solver. Meitner [4] used a computer program to analyze coolant flow in turbomachinery. Morris [5], experimentally, evaluated heat transfer in rotating coolant channels. Webb *et al.* [6] evaluated heat transfer and friction in tubes with rib turbulators, experimentally. Van Fossen [7] evaluated heat transfer coefficient for pin fins cooling by pins adding, experimentally. Chupp *et al.* [8] evaluated heat transfer coefficient for impingement cooling, experimentally. In 1987, Taslim [9] found experimentally friction factors and heat transfer coefficients in cooling passages of different aspect ratio. Furthermore, Taslim [10] in 1988 reported an experimental investigation on friction factors and heat transfer coefficients in passages of different aspect ratio roughened with turbulators. Johnson [11] experimentally evaluated effects of rotation on coolant passages. Kumar [12] developed a computer program for friction factor and heat transfer coefficient in rotating passages with rib turbulators and then compared the results with findings of Hajek *et al.* [13] which evaluated the effects of rotation on cooling channels.

The aims of current investigation are as follows: 1) general evaluation of cooling methods in radial turbine blades. 2) detailed analysis of tip-cap impingement cooling. 3) Use of bypass flow to accelerate trailing edges cooling. 4) Development of a computer program to analyze coolant flow on basis of momentum and energy equations. 5) Determination of critical points. 6) Comparison of obtained results with applied results of others. 7) Establishment of computing grid (Gambit) and run of the commercial CFD code (Fluent) in order to solve flow field and temperature in a stationary passage with area change and finned passage.

MODELING OF FLOW PATH AND CALCULATING PROCEDURES

Consider the flow of fluid through a control volume in a flow path rotating with speed N about an axis as shown in figure 2. The distance along the flow path is x and the distance from the rotation axis is r. Fluid is injected at a rate $d\dot{m}$ at velocity V_{inj}. The detailed momentum equation becomes:

$$(\dot{m}+d\dot{m})(V+dV)-(\dot{m}V+V_{inj,x}d\dot{m})= \\ pA+(p+\frac{dp}{2})dA-(p+dp)(A+dA)-\frac{\rho V^2 f 4A}{2D_h}dx+rN^2\rho A dr \tag{1}$$

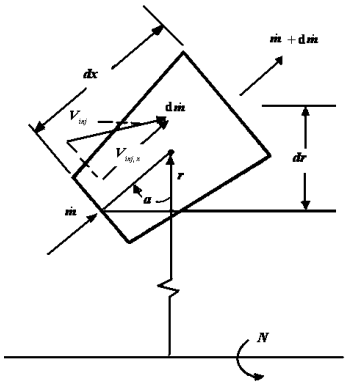

Figure 2. Control volume related to momentum equation

Consider the flow of fluid through the control volume shown in figure 3. Fluid is injected at a rate $d\dot{m}$ with a velocity V_{inj}. The detailed energy equation becomes:

$$(\dot{m}+d\dot{m})\left[h+dh+\frac{(V+dV)^2}{2}\right]-\left(h+\frac{V^2}{2}\right)\dot{m}-\left(h_{inj}+\frac{V_{inj}^2}{2}\right)d\dot{m}=h_c P dx(T_w-T_{aw}) \tag{2}$$

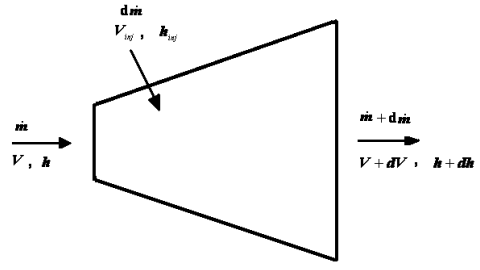

Figure 3. Control volume related to energy equation

(3) and (4) equations are two simultaneous equations in the variables (dT/dx) and (dp/dx). In order to march the pressure distribution and temperature distribution along the flow path they must be solved for the individual variables. After substituting the energy equation into the momentum equation and performing significant algebraic manipulation the final form of momentum equation, which is linear concerned to (dT/dx) takes the form shown as below:

$$\left(\frac{dp}{dx}\right)_n = \frac{1}{C_2}\left[\left\{C_1\left[\frac{\dot{m}}{C_p}\left(\frac{RT}{pA}\right)^2 + \frac{T}{\dot{m}} + \frac{\dot{m}}{2C_p}\left(\frac{RT}{pA}\right)^2 - \left(\frac{C_{p,inj}T_{inj}}{\dot{m}C_p} + \frac{V_{inj}^2}{2\dot{m}C_p}\right)\right]\right.\right.$$

$$\left.\left. + \frac{V_{inj,x}}{A} - \frac{2(\dot{m}/A)RT}{pA}\right\}\left(\frac{d\dot{m}}{dx}\right)_n + \left\{\frac{(\dot{m}/A)^2 RT}{pA} - \frac{C_1}{C_p A}\left(\frac{\dot{m}RT}{pA}\right)^2\right\}\left(\frac{dA}{dx}\right)_n\right.$$

$$\left. - \frac{4fRT(\dot{m}/A)^2}{2pD_h} + \frac{N^2 rp}{RT}\left(\frac{dr}{dx}\right) - \frac{4h_c AC_1(T_w - T_{aw})}{\dot{m}C_p D_h}\right] \tag{5}$$

Substituting equation (5) into equation (4), the final form of equation takes the form shown as below:

$$\left(\frac{dT}{dx}\right)_n = \frac{1}{C_T}\left[-\left\{\frac{\dot{m}}{C_p}\left(\frac{RT}{pA}\right)^2 + \frac{T}{\dot{m}} + \frac{\dot{m}}{2C_p}\left(\frac{RT}{pA}\right)^2 - \left(\frac{C_{p,inj}T_{inj}}{\dot{m}C_p} + \frac{V_{inj}^2}{2\dot{m}C_p}\right)\right\}\left(\frac{d\dot{m}}{dx}\right)_n\right.$$

$$\left. + \left\{\frac{1}{C_p A}\left(\frac{\dot{m}RT}{pA}\right)^2\right\}\left(\frac{dA}{dx}\right)_n + \left\{\frac{1}{pC_p}\left(\frac{\dot{m}RT}{pA}\right)^2\right\}\left(\frac{dp}{dx}\right)_n + \frac{4h_c A(T_w - T_{aw})}{\dot{m}C_p D_h}\right] \tag{6}$$

So that:

$$\left(\frac{d\dot{m}}{dx}\right)_n = \frac{(\dot{m}_n - \dot{m}_{n-1})}{l_n} \tag{7}$$

$$\left(\frac{dA}{dx}\right)_n = \frac{(A_n - A_{n-1})}{l_n} \tag{8}$$

$$\left(\frac{dr}{dx}\right)_n = \frac{(r_n - r_{n-1})}{l_n} \tag{9}$$

The constants C_1, C_2 and C_T are defined as follows:

$$C_1 = \frac{(\dot{m}/A)^2 R}{p\left[1 + \frac{(\dot{m}/A)^2 R^2 T}{p^2 C_p}\right]} \tag{10}$$

$$C_2 = 1 - \frac{(\dot{m}/A)^2 RT}{p^2} + \frac{C_1}{pC_p}\left[\frac{(\dot{m}/A)RT}{p}\right]^2 \tag{11}$$

$$C_T = 1 + \frac{(\dot{m}/A)^2 R^2 T}{p^2 C_p} \tag{12}$$

The flow path geometry is described in Cartesian coordinates at node points that, in turn, divide the flow path into a desired number of intervals. Each interval may be further subdivided into any desired number of slices to increase calculations accuracy. The nodes and intervals for the figure 1 upper flow path are shown in figure 4. From the inlet conditions and determined mass flow rate (guess), the flow solution is obtained by marching along the defined flow path from node to node. The pressure and temperature at each node are calculated from the previous node by :

$$p_n = p_{n-1} + \left(\frac{dp}{dx}\right)_n dx_n \tag{13}$$

$$T_n = T_{n-1} + \left(\frac{dT}{dx}\right)_n dx_n \tag{14}$$

$(dp/dx)_n$ and $(dT/dx)_n$ are obtained from solve of energy and momentum equations which derived from (5) and (6) correlations.

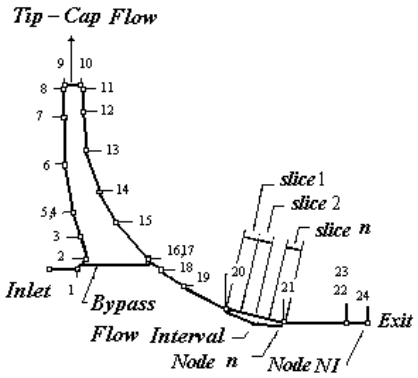

Figure 4. Nodal representation of figure 1 upper flow path

All calculations in this computer program are performing on basis of one dimensional compressible fluid flow which follows from perfect gas law. In order to analyze flow in this computer program, values by the following iterative procedure, consisting of an inner and outer iteration are calculated.
In order to get additional accuracy, the program further divides each input or slice interval into smaller sections called steps. During flow solution and marching along the defined flow path from step to step processes, convergence is occurred on mach number. This iteration procedure is referred to as the inner iteration. After calculation of pressure and temperature for all nodes, the amount of calculated pressure with determined pressure is compared in last node. If the relative differences between calculated and determined pressures became high, a new guess of inlet flow rate is then made and the marching procedure is repeated until the calculated and specified exit pressures converge. This iteration procedure is referred to as the outer iteration. If entrance pressure, entrance temperature and exit pressure; or entrance flow rate, entrance pressure and entrance temperature are selected as entry data, then, pressure distribution, temperature distribution, velocity distribution, local heat transfer coefficient, friction factor and local mass flow rate are calculated by the code and would be available to the designer. Standard correlations are used to predict the friction factor and heat transfer coefficient for each interval which is specified as being either a plain passage, a pin finned, a rib turbulator or a finned passage all are obtained from experimental correlations.

Plain Passages This kind of passages on the basis of size of diameter to roughness ratio (D/e_1) divided to two groups of smooth and rough passages and their related correlations of each group are effective in determination of friction factor.

Friction Factor. Correlations detailed in reference [4] are used for laminar flow, transition region and fully turbulent flow. A passage is considered to be smooth if the specified relative roughness is greater than 1×10^6. The detailed following formulas are used for laminar flow $(\mathrm{Re} \prec 2300)$, fully turbulent flow $(\mathrm{Re} \succ 3000)$ and transition region:
Laminar flow:

$$f = \frac{16}{\mathrm{Re}} \tag{15}$$

Fully turbulent flow:

$$\frac{1}{\sqrt{f}} = 1.737\left[(\mathrm{Re})\sqrt{f}\right] - 0.4 \tag{16}$$

Transition region:

$$f = \frac{\ln(\mathrm{Re}) - 7.271}{67.5144} \tag{17}$$

A passage is considered to be smooth if the specified relative roughness is more less than 1×10^6. The detailed following formulas are used for laminar flow $(\mathrm{Re} \prec 2300)$, fully turbulent flow $(\mathrm{Re} \succ 3000)$ and transition region:
Laminar flow:

$$f = \frac{16}{\mathrm{Re}} \tag{18}$$

Fully turbulent flow:

$$\frac{1}{\sqrt{f}} = 1.737 \ln\left(\frac{D}{e_1}\right) + 2.28 \tag{19}$$

This formula is valid for:

$$\frac{\left(\frac{D}{e_1}\right)}{(\mathrm{Re})\sqrt{f}} \prec 0.01$$

Transition region:

$$\frac{1}{\sqrt{f}} = 1.737 \ln\left(\frac{D}{e_1}\right) + 2.28 - 1.737 \left[\frac{4.67\left(\frac{D}{e_1}\right)}{(\mathrm{Re})\sqrt{f}} + 1\right] \tag{20}$$

This formula is valid for:

$$\frac{\left(\frac{D}{e_1}\right)}{(\mathrm{Re})\sqrt{f}} \geq 0.01$$

Heat Transfer Coefficient. The detailed following formulas for heat transfer coefficient are used for laminar flow $(\mathrm{Re} \prec 2300)$, fully turbulent flow $(\mathrm{Re} \succ 7000)$ and transition region:
Laminar flow:

$$h_{lam} = 4.226 \frac{K}{D_h} (\mathrm{Re})^{0.01} (\mathrm{Pr})^{0.333} \tag{21}$$

Fully turbulent flow:

$$h_{turb} = 0.023 \frac{K}{D_h} (\mathrm{Re})^{0.8} (\mathrm{Pr})^{0.333} \tag{22}$$

Transition region:

$$h_c = h_{lam} + \frac{h_{turb} - h_{lam}}{1 - e^{-2.951}} \times \left\{1 - \exp\left[\frac{-2.951(\mathrm{Re} - 2300)}{7000 - 2300}\right]\right\} \tag{23}$$

Equations (21), (22) and (23) were determined from a *J*-factor curve fit of data for a rectangular duct with a width to height ratio of 3.

Rib Turbulators In order to make a model for friction factor and heat transfer coefficient in circular or rectangular forms channels with rib turbulators, equations detailed in reference [6] are used. $(e_2/D), (\rho^+/e_2)$, Re and Pr describe the geometry for rib turbulators they are shown schematically in figure 5.

Friction Factor. For roughened tubes $(e^+ \succ 35)$, in a condition with $(10 \prec \rho^+/e_2 \prec 40)$, the friction factor is calculated below:

$$f = \frac{2}{\left[2.5 \ln\left(\frac{D}{2e_2}\right) - 3.75 + 0.95\left(\frac{\rho^+}{e_2}\right)^{0.53}\right]^2} \tag{24}$$

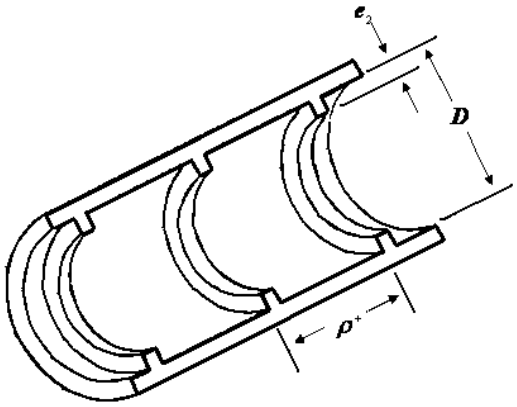

Figure 5. Rib Turbulators geometry

Heat Transfer Coefficient. Heat transfer coefficient is then evaluated from:

$$h_c = \frac{(St)(\mathrm{Re})(\mathrm{Pr})(K)}{D_h} \tag{25}$$

Where as:

$$St = \frac{\frac{f}{2}}{1+\left(\frac{f}{2}\right)^{0.5}\left[4.5\left(e^+\right)^{0.28}(\mathrm{Pr})^{0.57} - 0.95\left(\frac{\rho^+}{e_2}\right)^{0.53}\right]} \tag{26}$$

Pin-Fins For pin fins the correlation of Van Fossen [7] is used with hydraulic diameter and Reynolds number based on open volume:

$$(Nu)_v = 0.153(\mathrm{Re})_v^{0.685} \tag{27}$$

$$h_c = \frac{(Nu)_v K}{D_{h,v}} \tag{28}$$

Finned Passage In figure 6, a sketch of finned passage is shown. In flow passages with fins which are located parallel in flow direction (usually near to trailing edge), the transfer coefficient equation is collected from reference [4]:

$$h_c = \frac{h_{c,pp}}{W+\tau_f}\left[\frac{2\tanh\left(\varphi_f L_f\right)}{\varphi_f} + W\right] \tag{29}$$

$$\varphi_f = \left(\frac{2h_{c,pp}}{K\tau_f}\right)^{0.5} \tag{30}$$

$h_{c,pp}$ is the heat transfer coefficient for a plain passage obtained from equation (21).

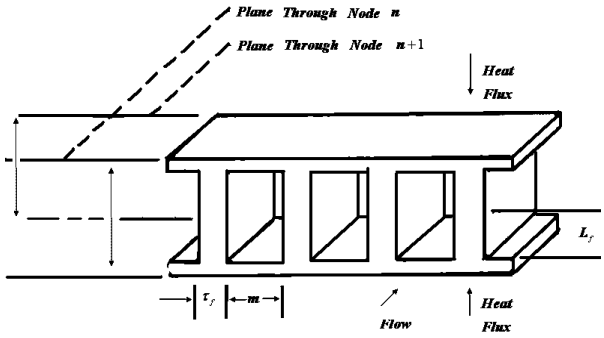

Figure 6. Finned passage geometry

Impingement Cooling The equations detailed in reference [8] were used for analyze of this kind of cooling. In figure 7,a sketch of tip cap geometry is shown. Station 2 represents the inlet holes, station 3 the impingement chamber at the exit of the inlet holes, and station 4 the impingement chamber at the entrance of the exit holes. Station 5, represents the exit holes. Heat transfer coefficients are obtained from equations as followed:

$$h_c = 0.63\left(\frac{K}{D_2}\right)(\mathrm{Re})_2^{0.7}\left[\frac{D_2}{(SP)_2}\right]^{0.5}\left(\frac{D_2}{D_4}\right)^{0.6}\times\exp\left[-1.27\left(\frac{L_{imp}}{D_4}\right)\left[\frac{D_2}{(SP)_2}\right]^{0.5}\left(\frac{D_2}{D_4}\right)^{1.2}\right] \tag{31}$$

The computer program in tip cap modeling would determine mass flow rate with consideration of jet holes.

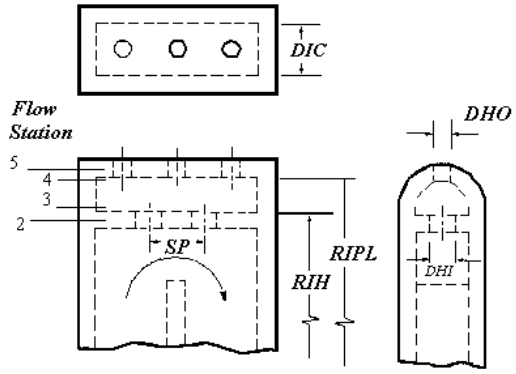

Figure 7. Tip cap geometry

Bypass Channel Simple equations of (5) and (6) are used, because of short length by pass channel and constant area change. The simplifications are the deletion of all heat transfer terms and the use of constant physical properties throughout.

Usage of Total Pressure Loss If the designer wanted to obtain some specific interval total pressure loss coefficient (K_T) it is transformed to a fanning friction factor as follows:

$$f = \frac{K_T D_h}{4l} \tag{32}$$

Calculating the total pressure loss due to sudden expansion or contraction by the resistance coefficients (K_T) for pipes. These resistance coefficients are based on the velocity in the smaller pipe and are defined by:

$$K_T = \frac{\Delta p}{\left(\frac{1}{2}\rho V^2\right)_{smaller\ \ pipe}} \tag{33}$$

For sudden expansion, the total pressure loss coefficient can be expressed analytically as:

$$K_T = \left(1 - \frac{A_1}{A_2}\right)^2 \tag{34}$$

Where A_1 is the inlet area and A_2 is the exit area. The curve for sudden contraction was curve fit by the following expressions:

$$X = \left(\frac{A_1}{A_2}\right)^{0.5} \tag{35}$$

$$K_T = -0.41468X^3 + 0.07014X^2 - 0.25946X + 0.5 \quad for \quad 0 \le X \prec 0.8 \tag{36}$$

$$K_T = 3.64583X^2 - 7.1875X + 3.54167 \quad for \quad 0.8 \le X \le 1 \tag{37}$$

Use of Colburn J-factor Curve If the Colburn J-factor curve defines in input program and designer want to put on the heat transfer coefficient in some special intervals by use of this curve, then the below formula get as follows:

$$h_c = \frac{j\rho V C_p}{(\mathrm{Pr})_F^{0.6667}} \tag{38}$$

Where, is the Prandtl number at the film temperature:

$$T_F = 0.5(T + T_w) \tag{39}$$

RESULTS

Pressure distribution, temperature distribution, velocity distribution, local heat transfer coefficient, friction factor and local mass flow rate along flow path show 1200*KPa* for inlet pressure and 637*K* for inlet temperature and 350*KPa* for exit pressure as shown in figures (8), (9), (10), (11), (12) and (13) in order of figures.

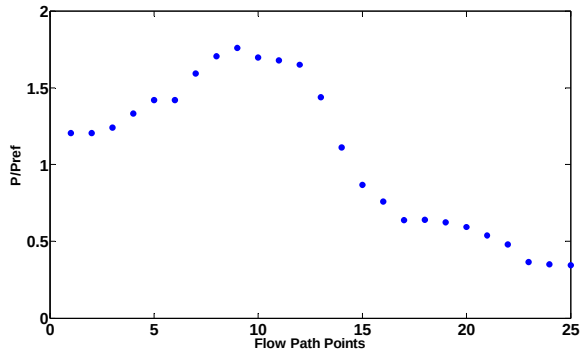

Figure 8. Pressure distribution along flow path

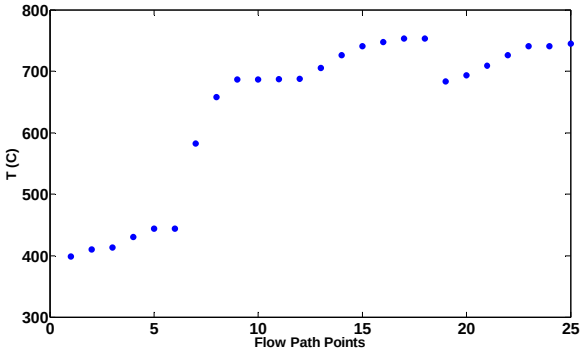

Figure 9. Temperature distribution along flow path

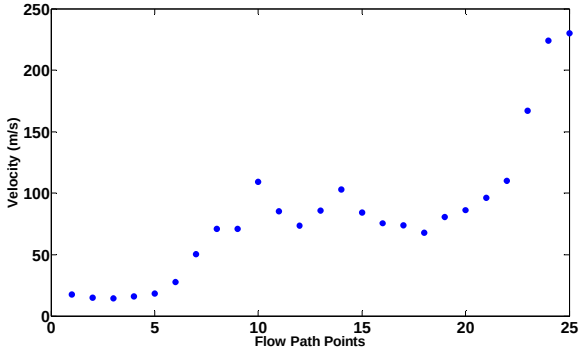

Figure 10. Velocity distribution along flow path

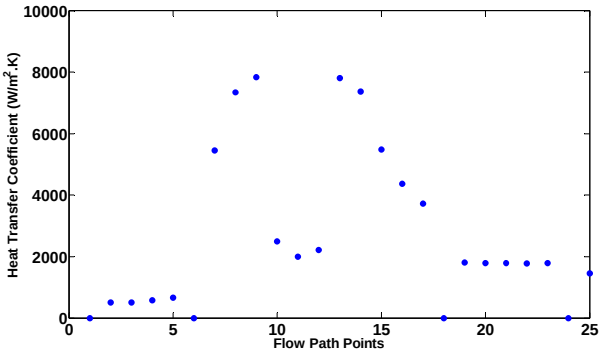

Figure 11. Heat transfer coefficient distribution along flow path.

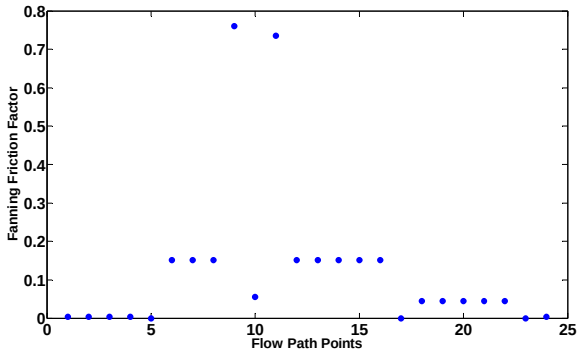

Figure 12. Friction factor distribution along flow path

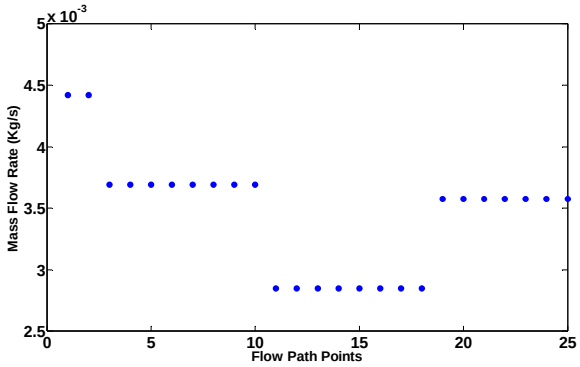

Figure 13. Mass flow rate distribution along flow path

Comparison of Variation of Heat Transfer Ratio Along Stationary Channel with Rotating Channel Comparison of heat transfer ratio for stationary and rotating conditions with consideration of smooth wall and rib turbulators are shown in figures (14) and (15). The noticeable point in these figures are: Relatively high amount of decline in heat transfer coefficient in the beginning of rotating channel in compare to stationary channel, and enhancement in heat transfer coefficient in ending part of rotating channel in compare to stationary channel.

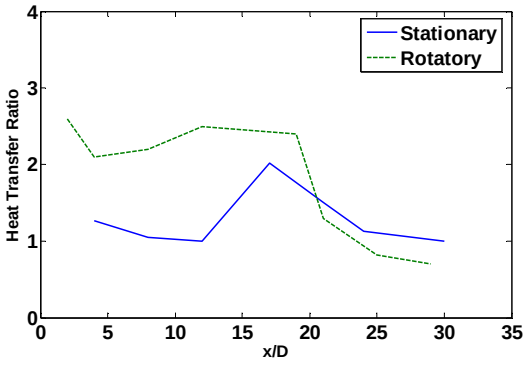

Figure 14. Variation of heat transfer ratio along stationary channel and rotating channel with smooth wall

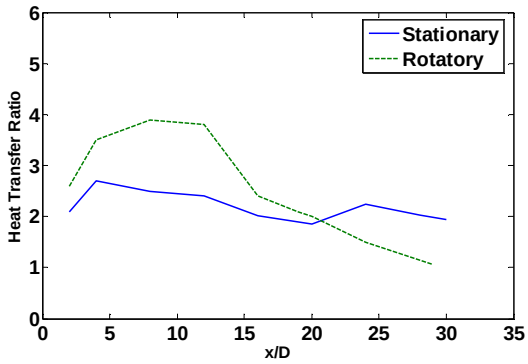

Figure 15. Variation of heat transfer ratio along stationary channel and rotating channel with rib turbulators.

Variations of Heat Transfer Ratio with Reynolds Number in Stationary Channel Variations of heat transfer ratio in stationary channel for Reynolds 12500, 25000 and 50000 are shown in figure (16). It is obvious that the heat transfer ratio for $\mathrm{Re}=12500$ is higher than those for the higher Reynolds numbers. This increase in heat transfer ratio is attributed to Reynolds number effects and heat transfer diminished by convection phenomenon and then caused decrease in heat transfer coefficient.

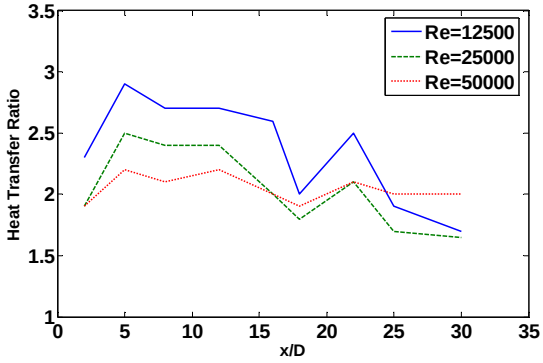

Figure 16. Variations of heat transfer ratio with Reynolds number in stationary channel

Variations of Heat Transfer Ratio with Reynolds Number in Rotating Channel Variations of heat transfer ratio in rotating channel for Reynolds 12500, 25000 and 50000 are shown in figure (17). Variation of heat transfer ratio is presented for a fixed rotation number ($Rs=0.12$). It is obvious that the heat transfer ratio for $\mathrm{Re}=12500$ is higher than those for the higher Reynolds numbers. This increase in heat transfer ratio is attributed to Reynolds number effects and heat transfer diminished by convection phenomenon and then caused decrease in heat transfer coefficient.

Variations of Heat Transfer Ratio with Rossby Number Along Channel The rotation number was varied from 0 to 0.35 for variations of heat transfer ratio along channel as shown in fig (18). Variation of heat transfer ratio is presented for a fixed $\mathrm{Re}=25000$. Observations indicated that heat transfer ratio for stationary channel significantly decreased and rotation was an affective factor on increasing of heat transfer coefficient.

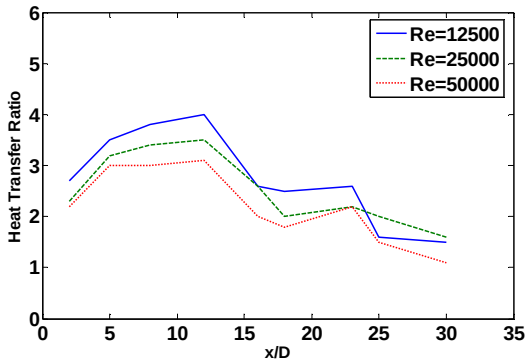

Figure 17. Variations of heat transfer ratio with Reynolds number in rotating channel

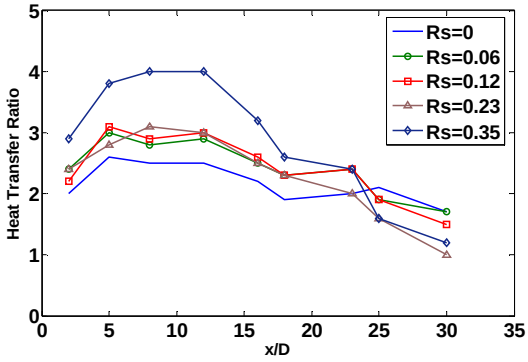

Figure 18. Variations of heat transfer ratio with Rotation number along channel

COMPARISON WITH EXPERIMENTAL DATA

In the following paragraphs, the predictions from the code are compared with a wide variety of experimental data for various types of heat transfer enhancement devices.
In a channel with rib turbulators, the obtained results from code, then compared with the experimental data of references (9) and (10), as shown in figures (19) and (20). Figure (19) compares the Nusselt number variation with Reynolds number for $\left(e_2/D=0.187\right)$ and $\left(\rho^+/e_2=10\right)$ in stationary channel. Figure (20) compares the heat transfer ratio with different ratios of rib height to hydraulic diameter for $\left(\rho^+/e_2=10\right)$ and $\mathrm{Re}=34000$.

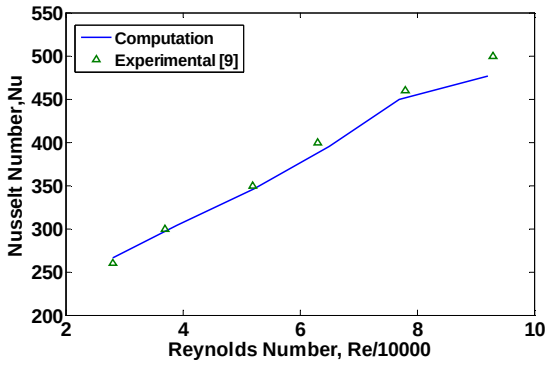

Figure 19. Variations of Nusselt number with Reynolds number along channel with rib turbulators

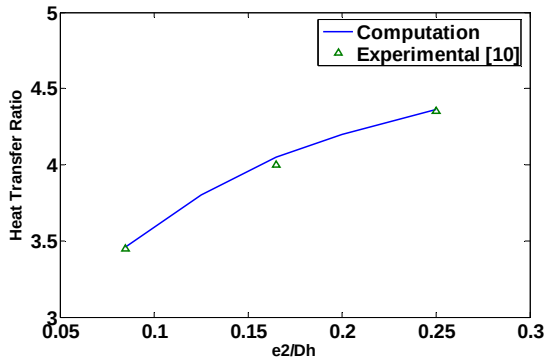

Figure 20. Variations of heat transfer ratio with different ratios of rib height to hydraulic diameter

Variation with Nusselt number along stationary channel with rib turbulators and smooth wall compared with the experimental data of reference (11), as shown in figures (21) and (22). In figure (21), variation with Nusselt number is presented for $(e_2/D = 0.145)$, $(\rho^+/e_2 = 10)$ and $\mathrm{Re} = 25176$. In figure (22), variation with Nusselt number is presented for smooth wall and $\mathrm{Re} = 25176$.

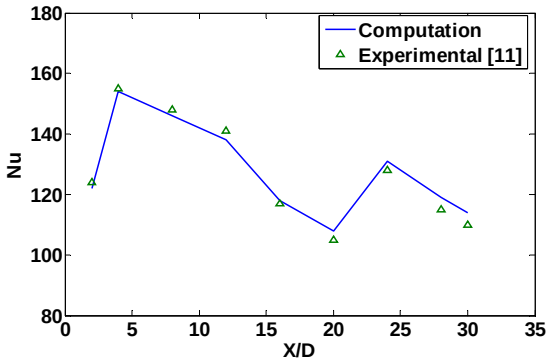

Figure 21. Variations of Nusselt number along stationary channel with rib turbulators

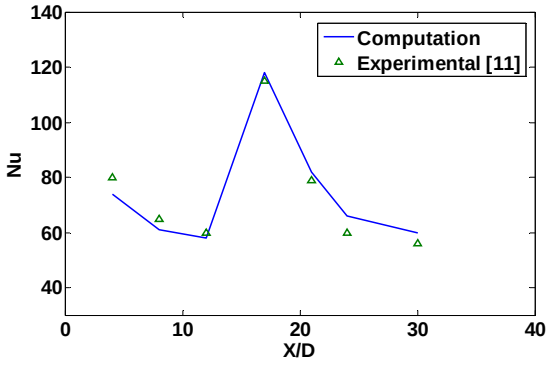

Figure 22. Variations of Nusselt number along stationary channel with smooth walls

Variation with Nusselt number along rotating channel with rib turbulators and smooth wall compared with the experimental data of reference (11), as shown in figures (23) and (24). In figure (23), variation with Nusselt number is presented for $N = 550rpm$, $(e_2/D = 0.145)$, $(\rho^+/e_2 = 10)$ and

$\mathrm{Re} = 24957$. In figure (24), variation with Nusselt number is presented for smooth wall, $N = 550 rpm$ and $\mathrm{Re} = 24957$.

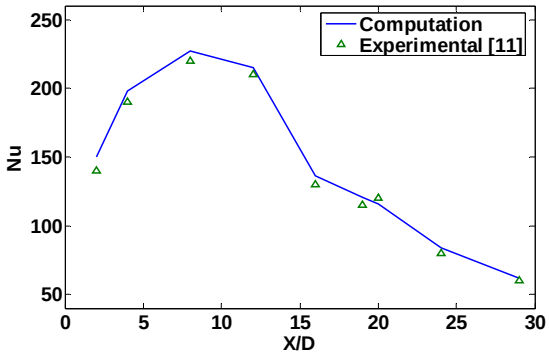

Figure 23. Variations of Nusselt number along rotating channel with rib turbulators

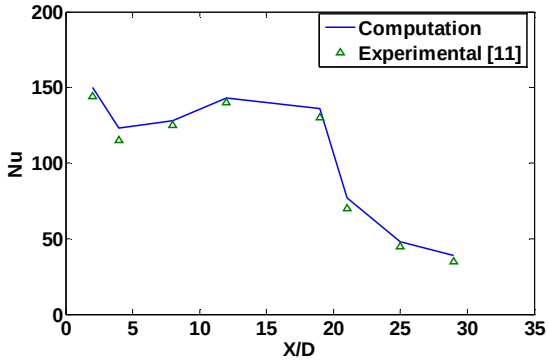

Figure 24. Variations of Nusselt number along rotating channel with smooth walls

Comparison of pressure variations along the passage with the data of reference (12) is shown in figure (25).

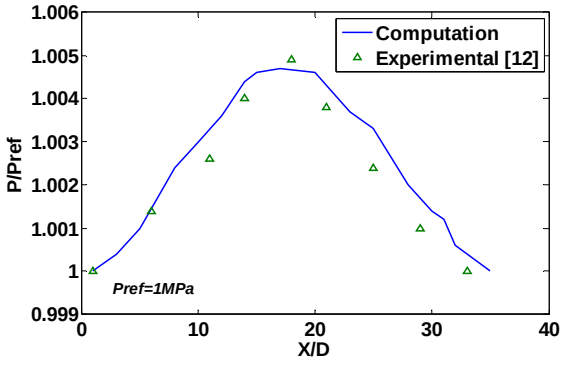

Figure 25. Variations of pressure along the passage

All the above figures clearly show that the code predictions agree well with the experimental data of others.

TWO-DIMENSIONAL NUMERAL ANALYSIS WITH THE CFD CODE

For this study a numerical code which contains control volume method was used. In order to discrete the terms of equations, one order approximate was used.
In this study, grids with (4000 & 6100 & 7200 & 8250) cells were examined. Selective grid of this complication, structure grid and uniformity was equal to 7200 cells. In four grids, the pressure distribution were compared and the results shown in figure (26). The results indicated that the selective grid became independent and recognized as a proper grid for analysis of problem with current code.
Inlet velocity boundary, wall boundary with constant temperature and outlet boundary were used for modeling of current investigation. The amount of Inlet velocity, inlet temperature, outlet temperature, wall temperature and rotation were: $10 m/s$, $300^{\circ}C$, $800^{\circ}C$ and $1200^{\circ}C$. Air properties consist of specific heat ratio, specific heat at constant pressure, viscosity and thermal conductivity were determined in the fluent code by author.

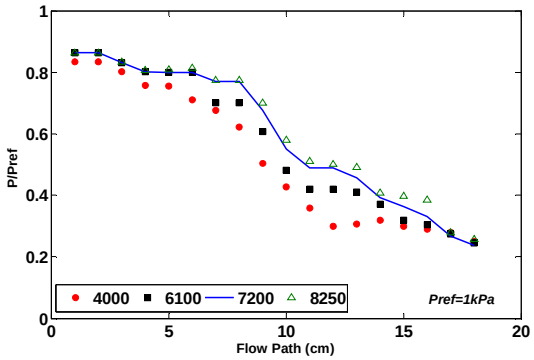

Figure 26. Effects of grid cells with pressure distribution along passage

Comparison of Results From Computer Code with CFD Code And Experimental Data In this section results of computer code and experimental data were compared with the obtained records of cfd code in center of flow. The comparison of pressure variations, temperature variations and velocity variations were shown in figures (27-29). All the above figures clearly show that the code predictions agree well with fluent code and the experimental data.

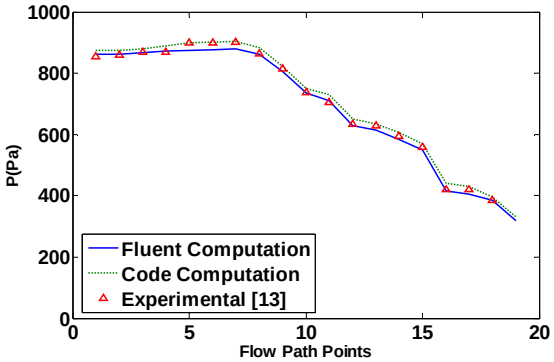

Figure 27. Comparison of pressure distribution from computer code with fluent and experimental data

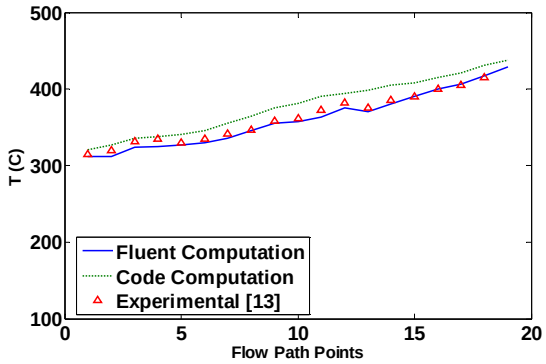

Figure 28. Comparison of Temperature distribution from computer code with fluent and experimental data

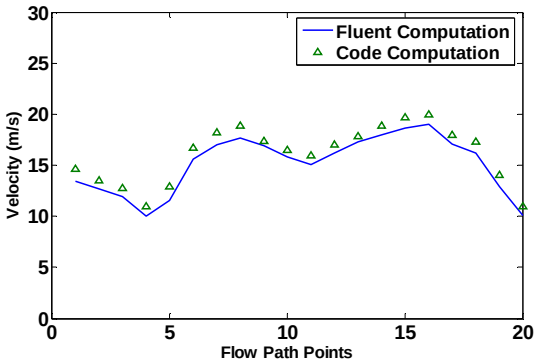

Figure 29. Comparison of velocity distribution from computer code with fluent data

CONCLUSION

In order to analyze cooling passage flow in radial turbine blades, a computer program was developed. This program would give an accurate image of the effects of designing parameters in cooling passages of turbine blade. It would be play an affective role in determination of critical points of radial turbine designing. The critical points are places with low heat transfer coefficient and high cooling fluid temperature. For this reason, heat transfer between cooling fluid and blade diminished and causes increase in blade temperature, which could affect on mechanical properties of blade alloy by damages. The designer would be supposed to modify different components of design by a manner to minimize the critical points of blade.

REFERENCES

El-wakill, M.M. [1985], Power Plant Technology, McGraw-Hill.

Steinthorsson, E., Liou, M.S., and Povinelli, L.A. [1993], Development of an Explicit Multiblock/Multigrid Flow Solver for Viscous Flows in Complex Geometries, AIAA-93-2380, Also:NASA TM-106356 and ICOMP 93-34.

Steinthorsson, E., Ameri, A.A., and Rigby, D.L. [1996], Simulations of Turbine Cooling Flows Using a Multiblock-Multigrid Scheme, NASA CR-198539, Also AIAA-96-0621 and ICOMP 96-7.

Meitner, P. [1990], Predicting Coolant Flow and Heat Transfer in Turbomachinery, NASA TP-2985, AVSCOM TP No. 89-C-008.

Morris, W.D. [1981], Heat Transfer and Fluid Flow in Rotating Coolant Channels, John Wiley & Sons.

Webb, R.L., Eckert, E.R., and Goldstein, R.J., [1971], Heat Transfer and Frictions in Tubes with Repeated-Rib Roughness, Int. J. Heat Mass Transfer, vol. 14, No. 4, pp. 601-617

Van Fossen, G.J, [1981], Heat Transfer Coefficients for Staggered Arrays of Short pin Fins, ASME Paper 81-GT-75

Chupp, R.E., et al., [1968], Evaluation of Internal Heat Transfer Coefficients for Impingement Cooled Turbine Airfoils, AIAA Paper 68-564

Taslim, M.E., and Spring, S.D., [1987], Friction Factors and Heat Transfer Coefficients in Turbulated Cooling Passages of Different Aspect ratio, Part One: Experimental results, Paper No. AIAA-87-2009, Presented at The AIAA/ASME/SAE/ASEE 23rd Joint Propulsion Conference, San Diego, California.

Taslim, M.E., and Spring, S.D., [1988], An Experimental Investigation of Heat Transfer Coefficients and Friction factors in Passages of Different Aspect Ratio Roughened with 450 Turbulators, Proceedings of the 1988 ASME National heat Transfer Conference, Huston, Texas, Vol. 1, pp. 661-668

Johnson, B.V., Wagner, J.H., and Steuber, G.D. [1993], Effects of Rotation on Coolant Passage Heat Transfer, NASA Contract Report No. NAS3-23691

Kumar, G.N., Roelke, R.J., and Meitner, P.L., [1989], A Generalized One Dimensional Computer Code for Turbomachinery Cooling Passage Flow Calculations", AIAA Paper 89-2574

Hajek, T.J., Wagner, J.H., and Johnson, B.V., [1987], Coolant Passage Heat Transfer with Rotation, Turbine Engine Hot Section Technology, NASA CP-2444, pp 211-223

Oosthuizen, P.H., Carascallen, W.E., [1997], Compressible Fluid Flow, McGraw-Hill

Sundberg, J. [2006], Heat Transfer Correlations for Gas Turbine Cooling, *M.Sc. Thesis*, Linkoping University Mech. Eng. Dept., Linkoping.